Journal of Geoscience and Environment Protection, 2024, 12, 198-214
https://www.scirp.org/journal/gep
ISSN Online: 2327-4344
ISSN Print: 2327-4336

Global Warming in Japanese Cities from 1960 to 2019 Using Machine Learning

Fumio Maruyama

Department of Sports and Health Science, Matsumoto University, Matsumoto, Japan
Email: fmaruya@nagoya-u.jp

How to cite this paper: Maruyama, F. (2024). Global Warming in Japanese Cities from 1960 to 2019 Using Machine Learning. *Journal of Geoscience and Environment Protection, 12,* 198-214.
https://doi.org/10.4236/gep.2024.129011

Received: August 28, 2024
Accepted: September 26, 2024
Published: September 29, 2024

Abstract

In this study, we investigated the variations in warming between Japanese cities for 1960-1989, and 1990-2019 using principal component analysis (PCA) and k-means clustering. The precipitation and sunshine hours exhibited opposite tendencies in the PCA results. It was found that 1960M and 1990M had a correlation (r = 0.51). The 1960M and 1990M are the mean temperature anomalies in Japanese cities for 1960-1989 and 1990-2019, respectively. There was a strong correlation between temperature and precipitation (r = 0.62). There was an inverse correlation between 1960M and sunshine hours (r = −0.25), but a correlation between 1990M and sunshine hours (r = 0.11). Sunshine hours had less effect on the 1960M but more impact on the 1990M. The k-means clustering for 1960M and 1990M can be classified into four types: high 1960M and high 1990M, which indicates that global warming is progressing rapidly (Sapporo, Tokyo, Kyoto, Osaka, Fukuoka, Nagasaki), low 1960M and low 1990M, global warming is progressing slowly (Nemuro, Ishinomaki, Yamagata, Niigata, Fushiki, Nagano, Karuizawa, Mito, Suwa, Iida, Hamada, Miyazaki, Naha), low 1960M and high 1990M, global warming has accelerated since 1990 (Utsunomiya, Kofu, Okayama, Hiroshima), and normal 1960M and normal 1990M, the rate of warming is normal among the 38 cities (Asahikawa, Aomori, Akita, Kanazawa, Maebashi, Matsumoto, Yokohama, Gifu, Nagoya, Hamamatsu, Kochi, Kagoshima). Higher annual temperatures were correlated with higher annual precipitation according to the k-means clustering of temperature and precipitation. Two of the four categories consisted of places with high annual temperatures and high precipitation (Fushiki, Kanazawa, Kochi, Miyazaki, Kagoshima, Naha, Ishigakijima), and places with low annual temperatures and low precipitation (Asahikawa, Nemuro, Sapporo, Karuizawa).

Keywords

Global Warming, Japan, Machine Learning, Principal Component Analysis, K-Means Clustering

1. Introduction

Changes in the Earth's climate since the mid-20th century have been driven by human activities, particularly fossil fuel burning, which increases heat-trapping greenhouse gas levels in the Earth's atmosphere and raises the Earth's average surface temperature (NASA, 2024). Natural processes that have been overwhelmed by human activities can also contribute to climate change, including internal variability (e.g., cyclical ocean patterns such as El Niño, La Niña, and Pacific Decadal Oscillation) and external forcing (e.g., volcanic activity, changes in the Sun's energy output, and variations in Earth's orbit).

Japan's average temperature varies widely from year to year, but over the long term, it has been on an upward trend, rising at a rate of 1.15˚C per 100 years, which is higher than the global average of 0.68˚C per 100 years. Both the number of extremely hot days with a maximum temperature of 35˚C and higher, and tropical nights with minimum temperatures of 25˚C and higher, appear to be on the rise. Changes in precipitation are also evident, with the number of days with rainfall of 1 mm or more declining, while the number of days with rainfall of 100 mm or more is increasing (JMA, 2012). According to the Automated Meteorological Data Acquisition System (AMeDAS) observations, the frequency of hourly heavy rains of 50 mm or more is extremely likely to have increased, although more data need to be collected before concluding whether there is any causal link between the trend and global warming.

The daily mean, maximum, and minimum temperatures for 59 years were analyzed from 1950 to 2008 using meteorological observation data from the Japan Meteorological Agency (Okochi & Yunokuchi, 2010). The annual average temperature of the 47 observatories in Japan is rising at a rate of 2.5/100 years. This includes global warming at 1.7/100 years and an urbanization effect at 0.8/100 years. Monthly mean temperatures showed a higher annual rate of increase.

Monthly temperature data for the period 1916-2010 in Japan were analyzed to quantitatively evaluate the background (non-urban) and urban warming trends (Fujibe, 2012). The results indicate that the warming trend of the background (non-urban) daily mean temperature was 0.88˚C/century averaged over the country, with a larger trend for the minimum temperature (1.21˚C/century) than for the maximum temperature (0.67˚C/century).

The temperature in the Northern Hemisphere has been rising rapidly since roughly 1990. As a result, we decided to investigate the change in temperature in the 30 years prior to and following 1990. In this study, we investigated the variations in warming between Japanese cities for 1960-1989, and 1990-2019 using principal component analysis (PCA) and k-means clustering.

2. Data and Analysis Methods

2.1. Data

The average annual precipitation, temperature, and sunshine hours in 38 Japanese cities from 1900 to 2019 obtained from the Automated Meteorological Data

Acquisition System (AMeDAS) provided by the Japan Meteorological Agency were used and listed in **Table 1**. The latitudes of the 38 AMeDAS observation points are listed. The 38 cities were chosen from AMeDAS locations throughout Japan to ensure a balanced distribution.

Table 1. Latitude, 1960M, 1990M, average annual temperature, rainfall, and sunshine hours at the AMeDAS observation points. The sites are listed from the highest to lowest latitudes.

Point	Latitude (˚)	1960M (˚C)	1990M (˚C)	Temp (˚C)	Rainfall (mm)	Sunshine hours (h)
Asahikawa	43.75	0.0956	0.941	7.2	1104.4	1566.5
Nemuro	43.33	−0.0630	0.701	6.6	1040.4	1846.7
Sapporo	43.06	0.170	1.255	9.2	1146.1	1718.0
Aomori	40.82	−0.0414	0.999	10.7	1350.7	1589.2
Akita	39.71	0.0362	1.007	12.1	1741.6	1527.4
Ishinomaki	38.42	−0.0294	0.674	11.9	1091.3	1946.7
Yamagata	38.25	−0.0270	0.892	12.1	1206.7	1617.9
Niigata	37.89	0.00177	0.886	13.9	1845.9	1639.6
Fushiki	36.79	0.0270	0.694	14.2	2281.0	1650.1
Nagano	36.66	−0.0144	0.814	12.3	965.1	1969.9
Kanazawa	36.58	0.0769	1.064	15.0	2401.5	1714.1
Karuizawa	36.54	−0.255	0.552	8.6	1246.2	2022.0
Utunomiya	36.54	−0.0532	1.231	14.3	1524.7	1961.1
Maebashi	36.40	0.0262	1.147	15.0	1247.4	2153.7
Mito	36.38	−0.0460	0.885	14.1	1367.7	2000.8
Matsumoto	36.24	0.0485	1.072	12.2	1045.1	2134.7
Suwa	36.04	−0.336	0.648	11.4	1301.5	2164.8
Tyoushi	35.73	−0.0850	0.730	15.8	1712.4	2017.8
Tokyo	35.69	0.394	1.377	15.8	1598.2	1926.7
Koufu	35.66	−0.113	1.122	15.1	1160.7	2225.8
Iida	35.52	−0.0432	0.787	13.1	1688.1	2074.5
Yokohama	35.43	0.0984	1.152	16.2	1730.8	2018.3
Gifu	35.40	0.102	1.171	16.2	1860.7	2108.6
Nagoya	35.16	−0.00240	1.181	16.2	1578.9	2141.0
Kyoto	35.01	0.303	1.236	16.2	1522.9	1794.1
Hamada	34.89	0.0328	0.732	15.7	1654.6	1761.3
Hamamatsu	34.75	−0.00283	0.941	16.8	1843.2	2237.9

Continued

Osaka	34.68	0.202	1.168	17.1	1338.3	2048.6
Okayama	34.68	−0.228	1.265	15.8	1143.1	2033.7
Hiroshima	34.39	−0.207	1.286	16.5	1572.2	2033.1
Matuyama	33.84	0.0774	1.097	16.8	1404.6	2014.5
Fukuoka	33.58	0.257	1.342	17.3	1686.9	1889.4
Kochi	33.56	0.0564	0.993	17.3	2666.4	2159.7
Nagasaki	32.73	0.310	1.055	17.4	1894.7	1863.1
Miyazaki	31.93	−0.0453	0.808	17.7	2625.5	2121.7
Kagoshima	31.55	0.0841	1.295	18.8	2434.7	1942.1
Naha	26.20	−0.0607	0.832	23.3	2161.0	1727.1
Ishigakijima	24.33	0.0187	0.719	24.5	2095.5	1852.5

2.2. Principal Component Analysis

Principal component analysis (PCA) attempts to recombine many original indexes with certain correlations into a new set of linearly independent comprehensive indexes to replace the original indexes. PCA is a method of identifying data patterns and expressing data in a manner that highlights their similarities and differences. PCA is a multivariate statistical data mining method used to reduce data size while preserving as many changes in the dataset as possible for faster and more efficient data processing (Jolliffe, 2011). Using PCA, many variables can be reduced to significantly important factors; thus, the resulting factors provide a summary of the original data. We performed PCA to derive climate indices that describe the main spatial features of the climate in Japanese cities using average annual precipitation, temperature, and sunshine hours for 1900-2019. PCA was performed using Python.

2.3. K-Means Clustering

The k-means clustering is a method of vector quantization, originally from signal processing, that aims to partition n observations into k clusters, in which each observation belongs to the cluster with the nearest mean (cluster centroid), serving as a prototype of the cluster. The k-means clustering method is widely used for weather classification owing to its simplicity and speed (Papadimitriou & Tsoukala, 2023). In this study, k-means clustering was performed using Python.

3. Results and Discussion

3.1 Global Warming in Japanese Cities

We estimated the average temperature anomalies of the 38 Japanese cities for 1960-1989 and 1990-2019 using average temperatures from 1900 to 2019. The calculation results for Tokyo are shown in **Figure 1(a)**. Changes in the temperature anomalies for 1960-1989 and 1990-2019 are shown in blue and red, respectively. The mean temperature anomalies were 0.394 and 1.377˚C for 1960-1989 (1960M) and 1990-2019 (1990M), respectively. Changes in temperature anomalies for 1940-1979 and 1980-2019 are shown in blue and red, respectively in Figure 1(b). The mean temperature anomalies were −0.00943 and 1.143˚C for 1940-1979 (1940M) and 1980-2019 (1980M), respectively.

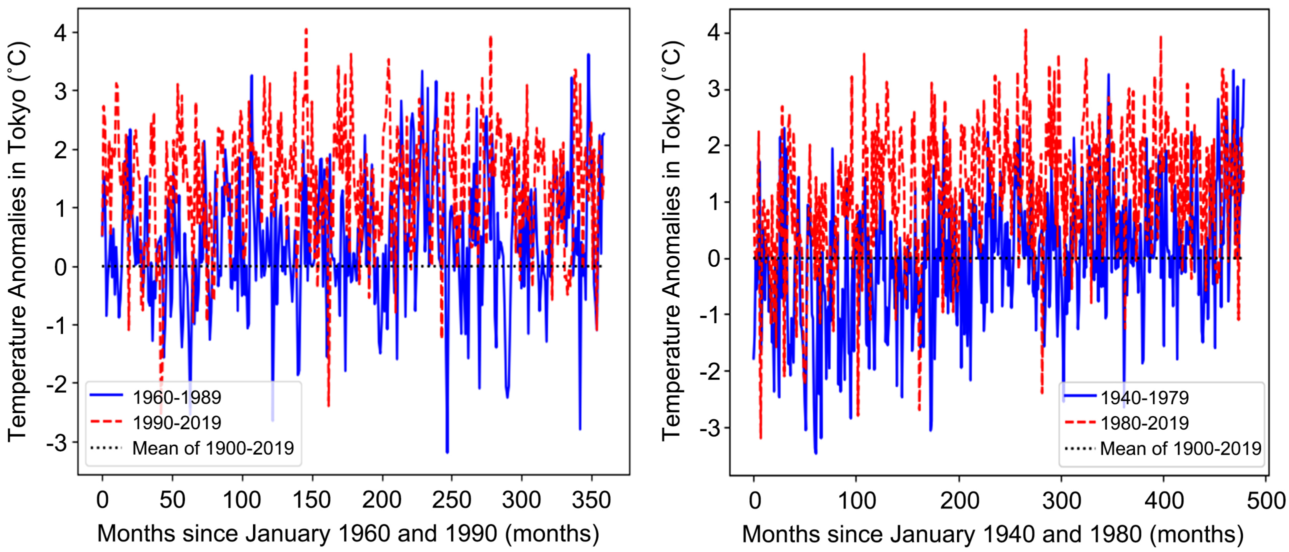

(a) (b)

Figure 1. (a) Changes in temperature anomalies for 1960-1989 and 1990-2019 in Tokyo. Mean temperature anomalies were 0.394 and 1.377˚C for 1960-1989 and 1990-2019, respectively; (b) Changes in temperature anomalies for 1940-1979 and 1980-2019 in Tokyo. Mean temperature anomalies were −0.00943 and 1.143˚C for 1940-1979 and 1980-2019, respectively.

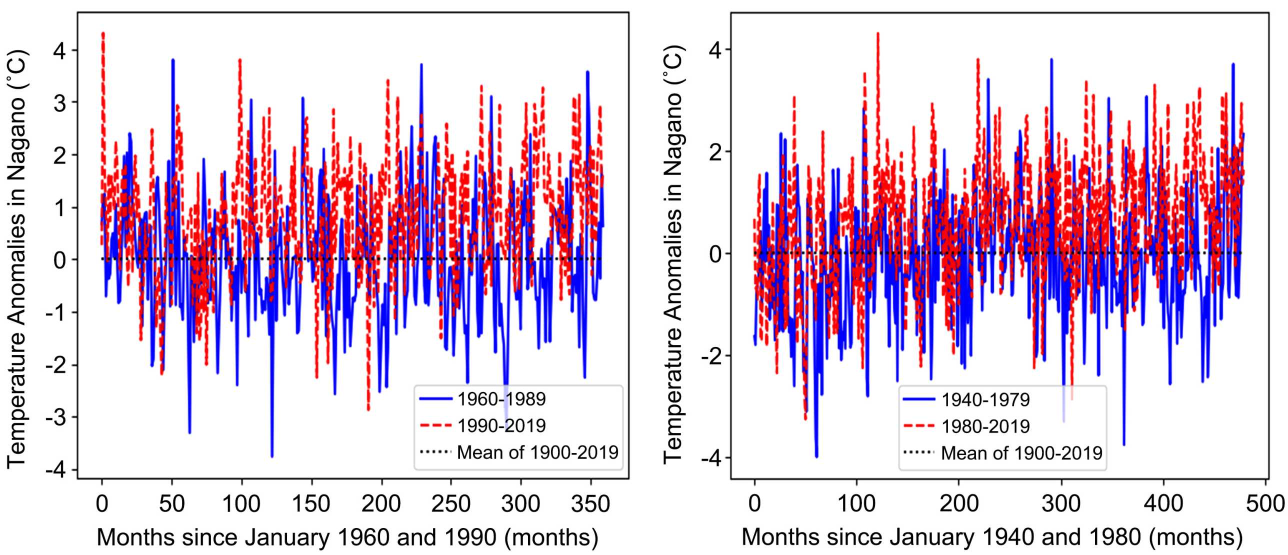

(a) (b)

Figure 2. (a) Changes in temperature anomalies for 1960-1989 and 1990-2019 in Nagano. Mean temperature anomalies were −0.0145 and 0.814˚C for 1960-1989 and 1990-2019, respectively; (b) Changes in temperature anomalies for 1940-1979 and 1980-2019 in Nagano. Mean temperature anomalies were −0.0969 and 0.592˚C for 1940-1979 and 1980-2019, respectively.

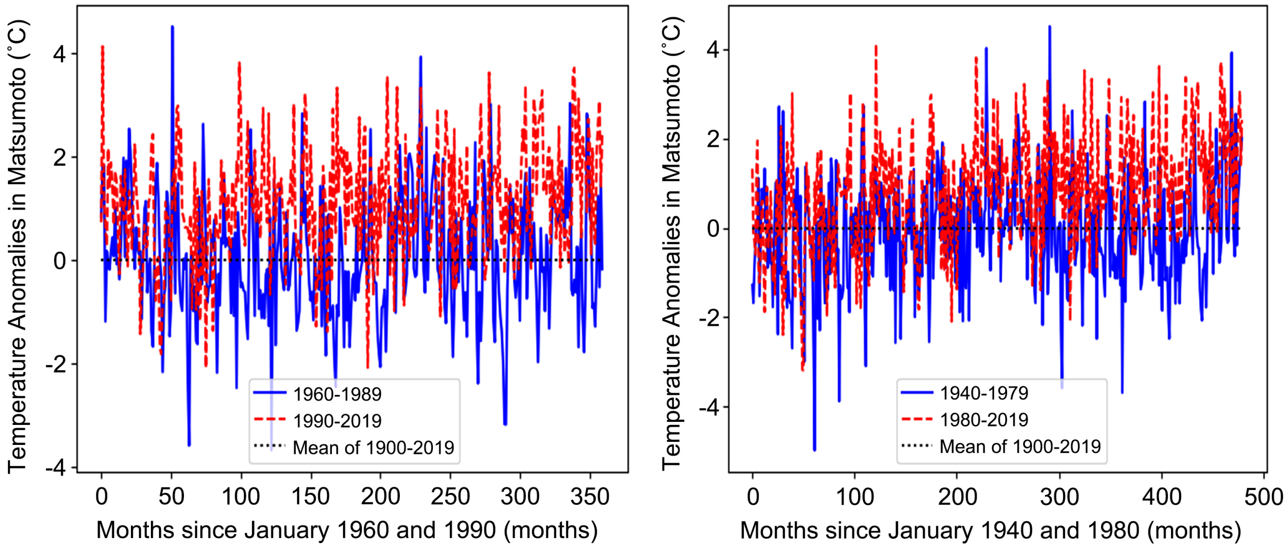

(a) (b)

Figure 3. (a) Changes in temperature anomalies for 1960-1989 and 1990-2019 in Matsumoto. Mean temperature anomalies were 0.0485 and 1.072˚C for 1960-1989 and 1990-2019, respectively; (b) Changes in temperature anomalies for 1940-1979 and 1980-2019 in Matsumoto. Mean temperature anomalies were −0.0487 and 0.814˚C for 1940-1979 and 1980-2019, respectively.

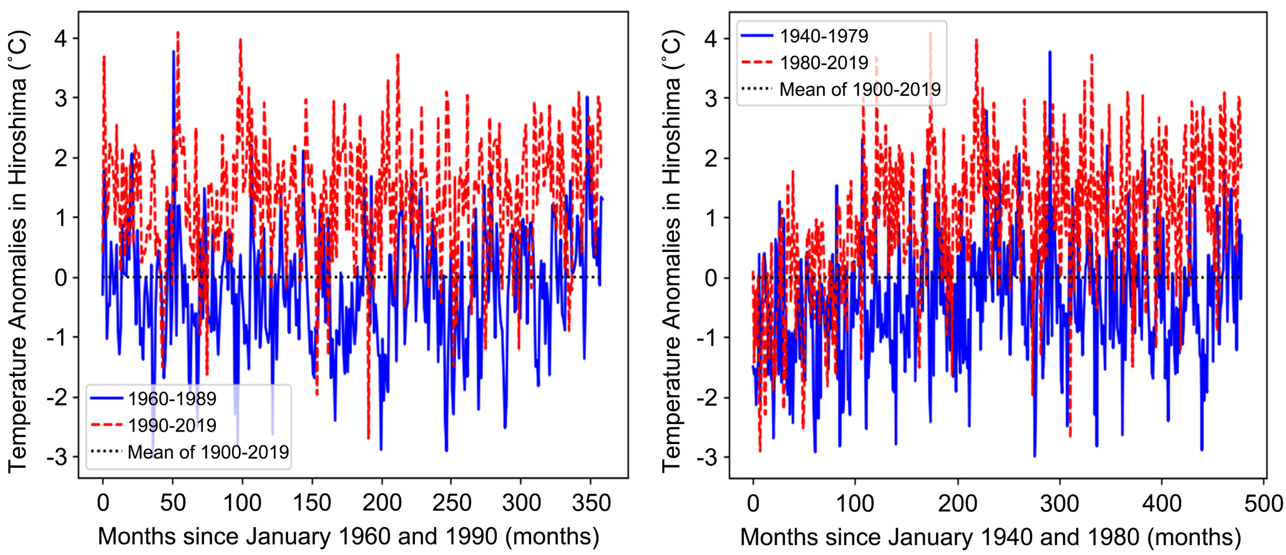

(a) (b)

Figure 4. (a) Changes in temperature anomalies for 1960-1989 and 1990-2019 in Hiroshima. Mean temperature anomalies were −0.207 and 1.286˚C for 1960-1989 and 1990-2019, respectively; (b) Changes in temperature anomalies for 1940-1979 and 1980-2019 in Hiroshima. Mean temperature anomalies were −0.411 and 0.940˚C for 1940-1979 and 1980-2019, respectively.

The calculation results for Nagano, Matsumoto, and Hiroshima are shown in Figure 2, Figure 3, and Figure 4, respectively. For every city, 1940M was negative. The 1960M for Nagano and Hiroshima was negative, and for Tokyo and Matsumoto, it was positive. For every city, 1980M and 1990M were positive. There was noticeable warming. The mean temperature anomalies for 1960-1989 (1960M) and 1990-2019 (1990M) are shown in Table 1.

3.2. Principal Component Analysis

The explained variances and loadings of the first two principal components calculated for 1960M, 1990M, annual precipitation, and sunshine hours for 1991-2020 in Japanese cities are shown in **Table 2(a)**. The first and second principal components account for 66.7% of the variance. **Figure 5** shows a principal component analysis (PCA) biplot diagram of 1960M, 1990M, average sunshine hours, and annual precipitation. The arrow indicates the relationship between each principal component and feature. The larger the dot product between the axis corresponding to the principal component and the arrow corresponding to the feature, the greater the correlation between the principal component and the feature. In the PCA results, the red arrows are nearly pointing in opposite directions; thus, precipitation and sunshine hours exhibit opposite tendencies. **Table 2(b)** shows the correlation between 1960M and 1990M (r = 0.51) and an inverse correlation between annual precipitation and sunshine hours (r = −0.03).

The explained variances and loadings of the first two principal components calculated for 1960M, annual temperature, sunshine hours, and precipitation in Japanese cities are shown in **Table 3(a)**. The first and second principal components account for 74.6% of the variance. **Figure 6** shows the PCA biplot diagram of 1960M, annual sunshine hours, temperature, and precipitation. In the PCA results, the red arrows are almost pointing in the opposite direction; therefore, the 1960M and sunshine hours have opposite trends. **Table 3(b)** shows the strong correlation between temperature and precipitation (r = 0.62) and an inverse correlation between 1960M and sunshine hours (r = −0.25).

The explained variances and loadings of the first two principal components calculated for 1990M, annual temperature, sunshine hours, and precipitation in Japanese cities are listed in **Table 4(a)**. The first and second principal components account for 70.4% of the variance. **Figure 7** shows the PCA biplot diagram of 1990M, annual sunshine hours, temperature, and precipitation. The red arrows of the 1990M and sunshine hours are parallel; therefore, the 1990M and sunshine hours follow the same trend. **Table 4(b)** shows the correlation between the 1990M and sunshine hours (r = 0.11).

The sunshine hours versus 1960M and 1990M are shown in **Figure 8**. When sunshine hours increased, 1960M increased and 1990M decreased. This corresponds to the negative correlation coefficient between 1960M and sunshine hours and a positive correlation coefficient between 1990M and sunshine hours.

The explained variances and loadings of the first two principal components calculated for 1960M, 1990M, 2000M, and 2010M in Japanese cities are shown in **Table 5(a)**. The 2000M and 2010M are the mean temperature anomalies for 2000-2009 and 2010-2019, respectively. The first and second principal components account for 92.5% of the variance. **Figure 9** shows a PCA biplot diagram of 1960M, 1990M, 2000M, and 2010M. The red arrows for 1990M, 2000M, and 2010 indicate almost the same direction; thus, they have the same trends and a strong correlation. **Table 5(b)** shows the correlation between 1960M and 1990M (r = 0.51).

Table 2. (a) Explained variances and loadings of the first two principal components calculated for 1960M, 1990M, annual sunshine hours, and precipitation in Japanese cities; (b) Correlation coefficients between the features.

(a)

	PC1	PC2
1960M (˚C)	−0.904	0.0726
1990M (˚C)	−0.762	−0.525
Sunshine hours (h)	0.262	−0.821
Annual precipitation (mm)	−0.305	0.390
Proportion of variance	0.390	0.277

(b)

1960M	1	0.51	−0.25	0.18
1990M	0.51	1	0.11	−0.01
Sunshine	−0.25	0.11	1	−0.03
Precipitation	0.18	−0.01	−0.03	1
	1960M	1990M	Sunshine	Precipitation

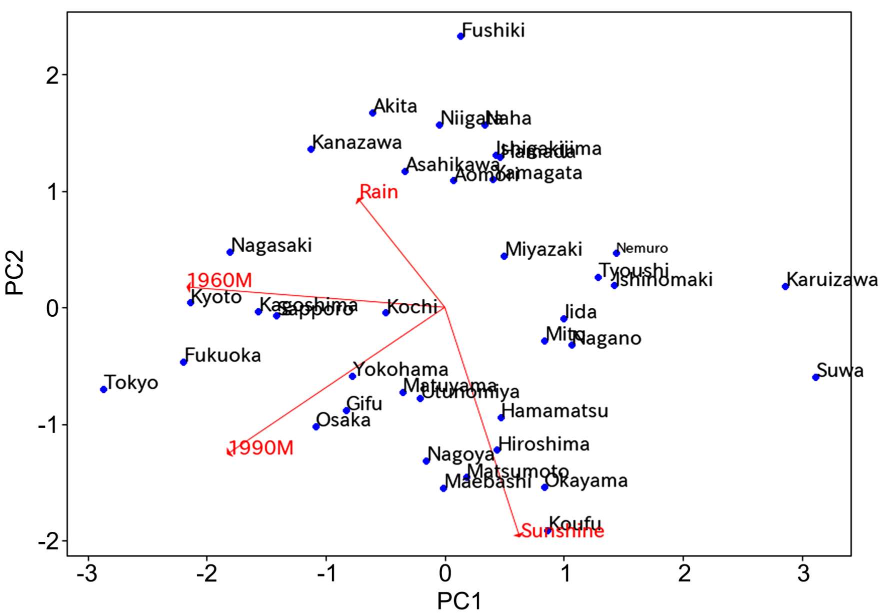

Figure 5. Principal component analysis (PCA) biplot diagram for 1960M, 1990M, average annual precipitation, and sunshine hours. The relationship between each principal component and each feature is indicated by an arrow. The larger the dot product between the axis corresponding to the principal component and the arrow corresponding to the feature, the greater the correlation between the principal component and the feature.

Table 3. (a) Explained variances and loadings of the first two principal components calculated for the 1960M, temperature, sunshine hours, and annual precipitation in Japanese cities; (b) Correlation coefficients between the features.

(a)

	PC1	PC2
1960M (˚C)	−0.443	−0.658
Temperature (˚C)	−0.888	0.238
Sunshine hours (h)	−0.0958	0.871
Annual precipitation (mm)	−0.860	−0.00374
Proportion of variance	0.434	0.312

(b)

1960M	1	0.21	−0.25	0.18
Temperature	0.21	1	0.23	0.62
Sunshine	−0.25	0.23	1	−0.03
Precipitation	0.18	0.62	−0.03	1
	1960M	Temperature	Sunshine	Precipitation

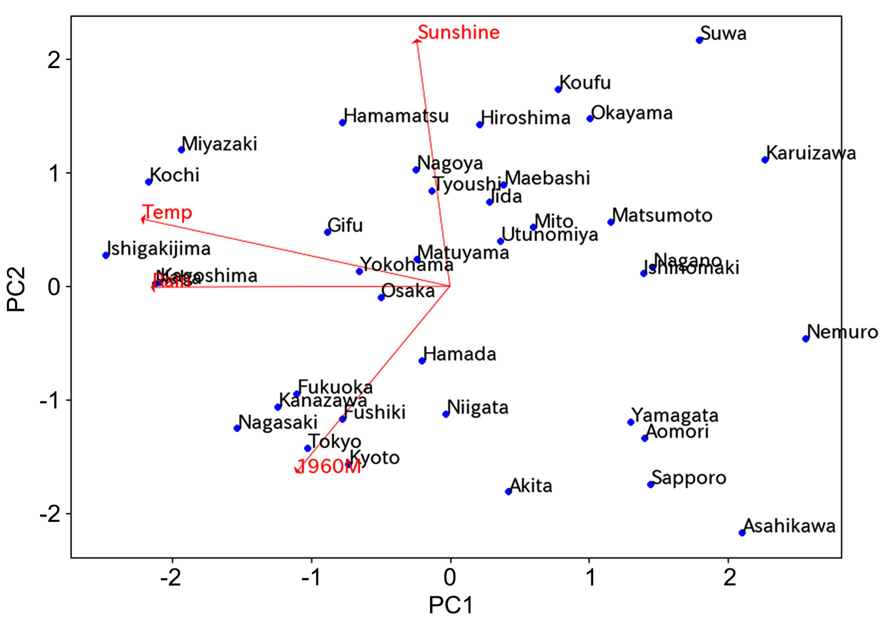

Figure 6. Principal component analysis (PCA) biplot diagram for 1960M, average annual precipitation, temperature, and sunshine hours. The relationship between each principal component and each feature is indicated by an arrow.

Table 4. (a) Explained variances and loadings of the first two principal components calculated for 1990M, temperature, sunshine hours, and annual precipitation in Japanese cities; (b) Correlation coefficients between the features.

(a)

	PC1	PC2
1990M (˚C)	0.351	−0.623
Temperature (˚C)	−0.920	0.0470
Sunshine hours (h)	−0.322	−0.684
Annual precipitation (mm)	−0.794	0.499
Proportion of variance	0.427	0.277

(b)

1990M	1	0.23	0.11	−0.01
Temperature	0.23	1	0.23	0.62
Sunshine	0.11	0.23	1	−0.03
Precipitation	−0.01	0.62	−0.03	1
	1990M	Temperature	Sunshine	Precipitation

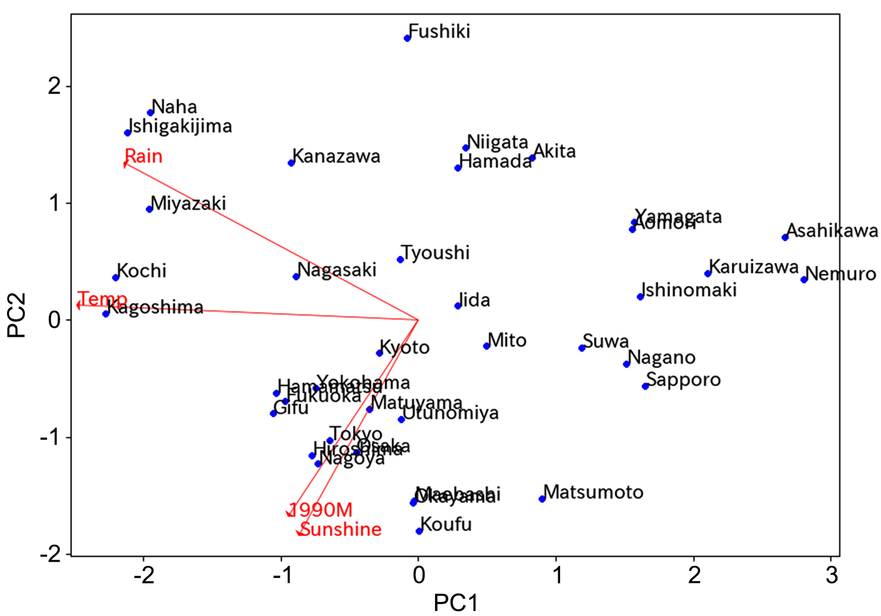

Figure 7. Principal component analysis (PCA) biplot diagram for 1990M, average annual precipitation, temperature, and sunshine hours. The relationship between each principal component and each feature is indicated by an arrow.

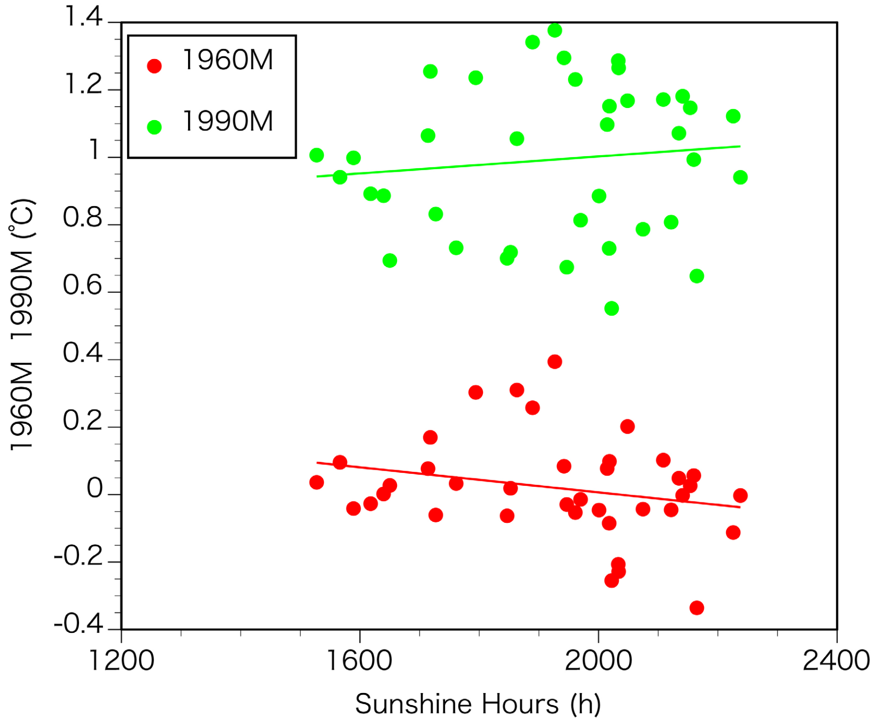

Figure 8. Sunshine hours versus 1960M and 1990M.

Table 5. (a) Explained variances and loadings of the first two principal components calculated for 1960M, 1990M, 2000M, and 2010M in Japanese cities; (b) Correlation coefficients between the features.

(a)

	PC1	PC2
1960M (˚C)	−0.652	−0.757
1990M (˚C)	−0.979	0.171
2000M (˚C)	−0.923	0.130
2010M (˚C)	−0.891	0.231
Proportion of variance	0.758	0.168

(b)

1960M	1	0.51	0.49	0.42
1990M	0.51	1	0.94	0.89
2000M	0.49	0.94	1	0.72
2010M	0.42	0.89	0.72	1
	1960M	1990M	2000M	2010M

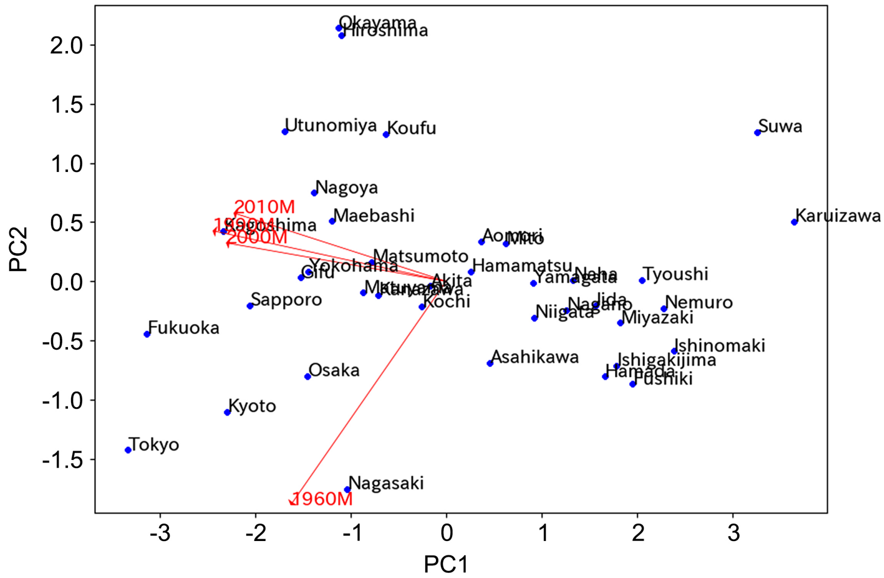

Figure 9. Principal component analysis (PCA) biplot diagram for 1960M, 1990M, 2000M, and 2010M. The relationship between each principal component and each feature is indicated by an arrow.

3.3. K-Means Clustering Analysis

The k-means clustering of the longitude and latitude of the 38 AMeDAS observation points is shown in **Figure 10**. It nearly resembles Japan in shape.

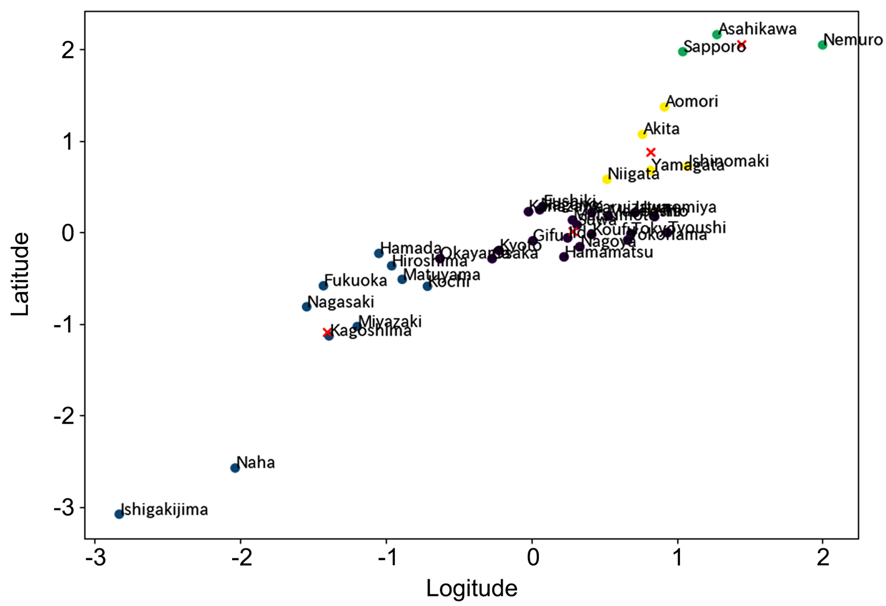

Figure 10. The k-means clustering of longitude and latitude of the 38 AMeDAS observation points. × is cluster centroid.

The k-means clustering of the 1960M and 1990M is shown in **Figure 11**. It can be classified into four types: high 1960M and high 1990M, which indicates that global warming is progressing rapidly (Sapporo, Tokyo, Kyoto, Osaka, Fukuoka, Nagasaki), low 1960M and low 1990M, global warming is progressing slowly (Nemuro, Ishinomaki, Yamagata, Niigata, Fushiki, Nagano, Karuizawa, Mito, Suwa, Iida, Hamada, Miyazaki, Naha), low 1960M and high 1990M, global warming has accelerated since 1990 (Utsunomiya, Kofu, Okayama, Hiroshima), and normal 1960M and normal 1990M, the rate of warming is normal among the 38 cities (Asahikawa, Aomori, Akita, Kanazawa, Maebashi, Matsumoto, Yokohama, Gifu, Nagoya, Hamamatsu, Kochi, Kagoshima).

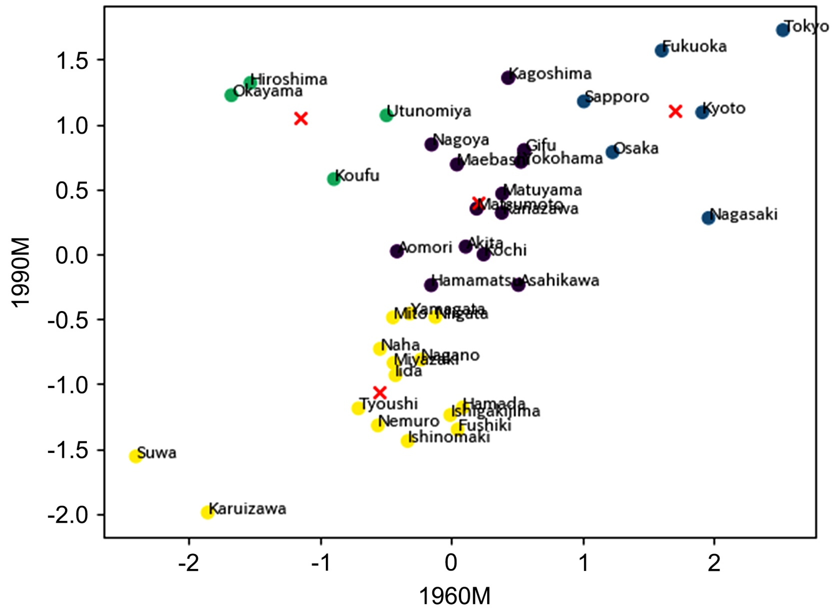

Figure 11. The k-means clustering of 1960M and 1990M. × is cluster centroid.

The k-means clustering of latitude and 1990M is shown in Figure 12. The 1990M was distributed at mid-latitudes. This is due to the fact that it contains the high-altitude cities of Iida (516 m), Suwa (760 m), Karuizawa (999 m), and Nagano (418 m). Although Naha and Ishigakijima are located at low latitudes, 1990M is not large.

It is possible to classify the k-means clustering of the 2000M and 2010M; the larger the 2000M, the larger the 2010M. The 2000M and 2010M at each point increase at a similar rate.

The k-means clustering of latitude and temperature is shown in Figure 13. It is evident that the lower the latitude, the higher the temperature. It can be classified into four types: high latitude and low temperature (Asahikawa, Nemuro, Sapporo, Aomori, Akita), low latitude and high temperature (Miyazaki, Naha, Ishigakijima), normal latitude and normal temperature (Tokyo, Nagoya, Osaka, Hiroshima, Fukuoka, etc.), and normal latitude and distributed temperature (Niigata, Mito, Nagano, Karuizawa, Suwa, Iida, etc.).

The highest points were Nagano (418 m), Karuizawa (999 m), Suwa (760 m), and Iida (516 m). Compared with other locations in the same latitude, the temperature was lower at these highest points.

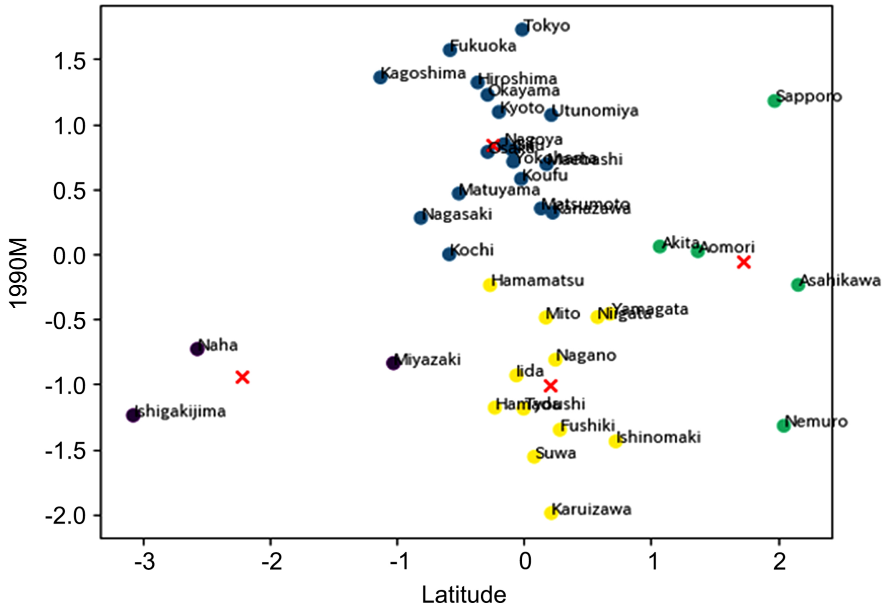

Figure 12. The k-means clustering of latitude and 1990M. × is cluster centroid.

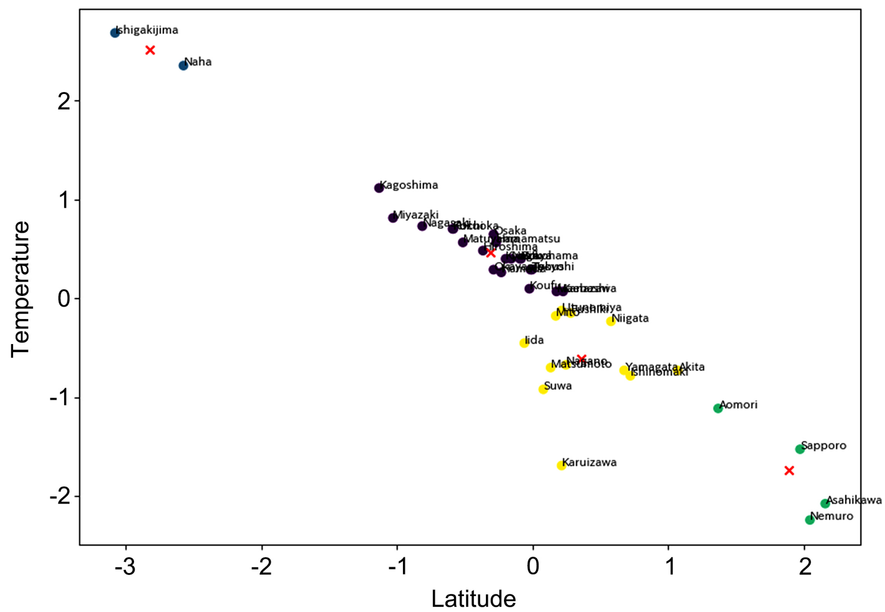

Figure 13. The k-means clustering of latitude and temperature. × is cluster centroid.

The k-means clustering of temperature and precipitation is shown in Figure 14. The higher the annual temperature, the greater the annual precipitation. The locations were classified into four categories: locations with high annual temperature and high precipitation (Fushiki, Kanazawa, Kochi, Miyazaki, Kagoshima, Naha, Ishigakijima), locations with normal annual temperature and normal precipitation (Akita, Niigata, Utsunomiya, Iida, Tyoushi, Tokyo, Yokohama, Gifu, Hamamatsu, Kyoto, Hamada, Osaka, Hiroshima, Matsuyama, Fukuoka, Nagasaki), locations with a little low annual temperature and a little low precipitation (Aomori, Ishinomaki, Yamagata, Nagano, Maebashi, Mito, Matsumoto, Suwa, Kofu, Okayama), and locations with low annual temperature and low precipitation (Asahikawa, Nemuro, Sapporo, Karuizawa).

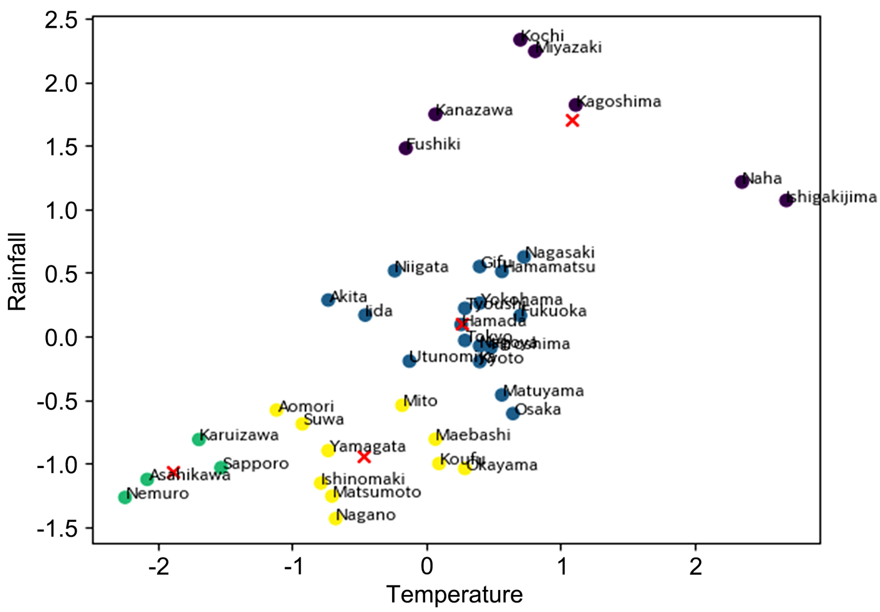

Figure 14. The k-means clustering of temperature and rainfall. × is cluster centroid.

The k-means clustering of sunshine hours and 1960M, 1990M are shown in Figure 15 and Figure 16, respectively. The 1990M values are more widely distributed and depend more on sunshine hours. The 1960M is less affected by sunshine hours, whereas the 1990M is more affected. Okayama and Hiroshima are two examples of the long sunshine hours relative to 1960M. However, because Karuizawa and Suwa are higher up, 1960M is less.

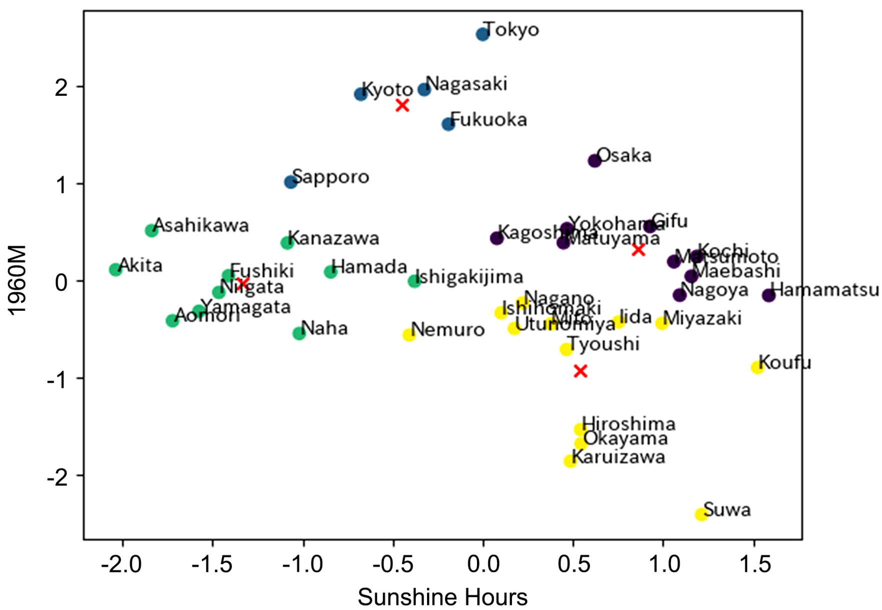

Figure 15. The k-means clustering of sunshine hours and 1960M. × is cluster centroid.

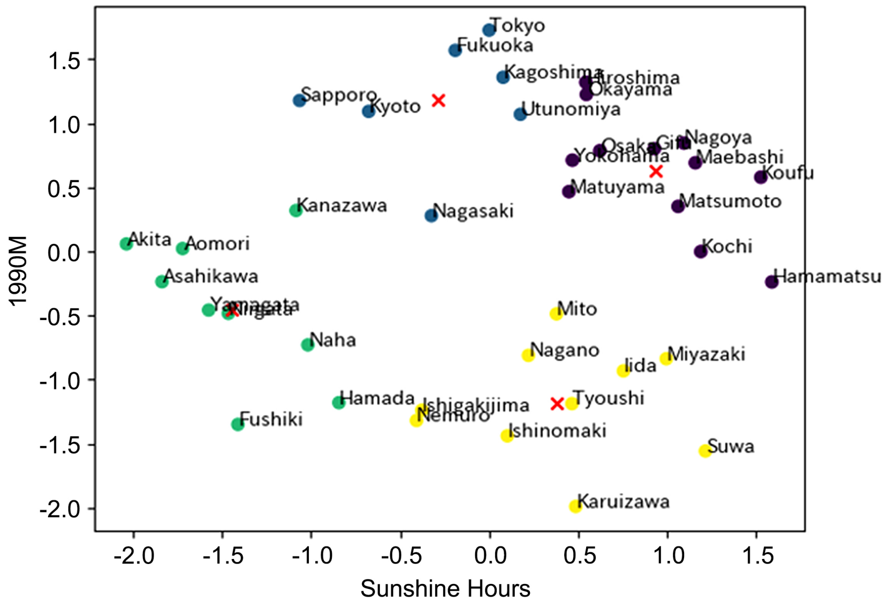

Figure 16. The k-means clustering of sunshine hours and 1990M. × is cluster centroid.

4. Conclusion

In this study, we investigated the variations in warming between Japanese cities for 1960-1989, and 1990-2019 using principal component analysis (PCA) and k-means clustering.

1) The precipitation and sunshine hours exhibited opposite tendencies in the PCA results. It was found that 1960M and 1990M had a correlation (r = 0.51). The 1960M and 1990M are the mean temperature anomalies in Japanese cities for 1960-1989 and 1990-2019, respectively. There was a strong correlation between temperature and precipitation (r = 0.62). There was an inverse correlation between 1960M and sunshine hours (r = −0.25), but a correlation between 1990M and sunshine hours (r = 0.11). Sunshine hours had less effect on the 1960M but more impact on the 1990M.

2) The k-means clustering for 1960M and 1990M can be classified into four types: high 1960M and high 1990M, which indicates that global warming is progressing rapidly (Sapporo, Tokyo, Kyoto, Osaka, Fukuoka, Nagasaki), low 1960M and low 1990M, global warming is progressing slowly (Nemuro, Ishinomaki, Yamagata, Niigata, Fushiki, Nagano, Karuizawa, Mito, Suwa, Iida, Hamada, Miyazaki, Naha), low 1960M and high 1990M, global warming has accelerated since 1990 (Utsunomiya, Kofu, Okayama, Hiroshima), and normal 1960M and normal 1990M, the rate of warming is normal among the 38 cities (Asahikawa, Aomori, Akita, Kanazawa, Maebashi, Matsumoto, Yokohama, Gifu, Nagoya, Hamamatsu, Kochi, Kagoshima).

3) Higher annual temperatures were correlated with higher annual precipitation according to the k-means clustering of temperature and precipitation. Two of the four categories consisted of places with high annual temperatures and high precipitation (Fushiki, Kanazawa, Kochi, Miyazaki, Kagoshima, Naha,

Ishigakijima), and places with low annual temperatures and low precipitation (Asahikawa, Nemuro, Sapporo, Karuizawa).

Conflicts of Interest

The author declares no conflicts of interest regarding the publication of this paper.

References

Fujibe, F. (2012). Evaluation of Background and Urban Warming Trends Based on Centennial Temperature Data in Japan. *Meteorology and Geophysics, 63,* 43-56. https://doi.org/10.2467/mripapers.63.43

Jolliffe, I. (2011). Principal Component Analysis. In *International Encyclopedia of Statistical Science* (pp. 1094-1096). Springer. https://doi.org/10.1007/978-3-642-04898-2_455

NASA (2024). https://science.nasa.gov/climate-change/what-is-climate-change/

Okochi, Y., & Yunokuchi, T. (2010). Urban and Global Warming in Japan. *Research Reports of Kumamoto-NCT, 2*.

Papadimitriou, A., & Tsoukala, V. (2023). Evaluating and Enhancing the Performance of the K-Means Clustering Algorithm for Annual Coastal Bed Evolution Applications. *Oceanologia, 66,* 267-285. https://doi.org/10.1016/j.oceano.2023.12.005

The Japan Meteorological Agency (JMA) (2012). *Climate Change Monitoring Report 2011.*